Nat. Hazards Earth Syst. Sci. Discuss., 3, 6977–6996, 2015
www.nat-hazards-earth-syst-sci-discuss.net/3/6977/2015/
doi:10.5194/nhessd-3-6977-2015

Natural Hazards and Earth System Sciences
Discussions
Open Access

Evaluating flood potential with GRACE in the United States

T. Molodtsova[1], S. Molodtsov[1], A. Kirilenko[2], X. Zhang[2], and J. VanLooy[2]

[1]Texas A and M University, College Station, Texas, USA
[2]University of North Dakota, Grand Forks, North Dakota, USA

Received: 18 October 2015 – Accepted: 24 October 2015 – Published: 19 November 2015

Correspondence to: T. Molodtsova (tatiana.molodtsova@gmail.com)

Published by Copernicus Publications on behalf of the European Geosciences Union.

Abstract

One of the Gravity Recovery and Climate Experiment (GRACE) products, the Terrestrial Water Storage Anomaly (TWSA), was used for assessing large-scale flood risk through Reager's Flood Potential Index (RFPI) by Reager and Famiglietti (2009). The efficacy of the proposed RFPI for flood risk assessment was evaluated over the continental US using multi-year flood observation data from 2003 to 2012 by the US Geological Survey and Dartmouth Flood Observatory. In general, the flood risk based on the RFPI agreed well with the observed floods on regional and even local scales. The method exhibits higher skill in predicting the large-area, long-duration floods, especially during the summer season.

1 Introduction

Globally, floods rank first in natural disasters by the total number of people affected and the cost (Center for Research on the Epidemiology of Disasters, 2013). Intensive precipitation events have increased during the final decades of the 20th century (Groisman et al., 2005; Alexander et al., 2006; Trenberth, 2011) and are expected to further intensify in the future (Groisman, 2012). In response, many countries have developed flood alert systems, such as the European Flood Alert System (Bartholmes, 2009) and the National Weather Service Automated Flood Warning System (Scawthorn, 1999) in the United States. While most of the systems rely on a dense network of gage stations, over 95 % of all deaths and a significant part of the economic losses caused by floods occur in developing countries where ground flood monitoring and management programs are still inefficient, and the costs of building control infrastructure such as dams, weirs, embankments, and gage stations can be prohibitive (Tariq, 2011). These problems were well demonstrated during the 2010 flood disaster in Pakistan (Larkin, 2010) where the deficiencies in flood monitoring and the ensuing lack of information led

NHESSD
3, 6977–6996, 2015

to coordination chaos (Hagen, 2011) and contributed towards an estimated $35 billion (US) loss in economic impact.

To compensate for or complement the ground based observations, flood monitoring is increasingly using the products obtained with remote sensors such as NASA's AMSR-E (Wang et al., 2003), Quick Scatterometer (QuickSCAT) (Brakenridge et al., 2003), Spinning Enhanced Visible and InfraRed Imager (SEVIRI) (Proud et al., 2011), and Moderate Resolution Imaging Spectroradiometer (MODIS) (Brakenridge and Anderson, 2006). Among the remote sensing products that have been used for flood monitoring, data from the Gravity Recovery and Climate Experiment (GRACE) (Adam, 2002; Chen et al., 2004) is unique in that the changes in the amount of terrestrial water are directly measured. Reager and Famiglietti (2009) used a GRACE-derived Total Water Storage Anomaly (TWSA) product together with precipitation data to estimate flood risks worldwide. They combine past variations in total water storage with the record of recent precipitation to generate Reager's Flood Potential Index (RFPI). A qualitative comparison of calculated RFPI with the Dartmouth Flood Observatory (DFO) dataset of historic floods showed that the GRACE gravitational data in general and the proposed RFPI product in particular are useful for flood risk assessment in most regions. However no quantitative validation results were reported. This leads to the main objective of our study: evaluate the skill of RFPI for flood forecasting over the continental US, where floods are routinely monitored.

2 Data and methodology

2.1 Flood Potential Index

The concept of RFPI is explained in detail in Reager and Famiglietti (2009). Briefly, the historical TWSA from GRACE provides an estimate of the range of the amount of water a region can hold, or storage deficit; and flood risk is estimated by comparing precipitation with this range. The values of RFPI vary from $-\infty$ and 1, with positive values indicating that water input from precipitation is above the mean water storage and should be interpreted as a potential risk for flooding. The GRACE Release-5 10/2012 TWSA product (Adam, 2002) and CPC Merged Analysis of Precipitation (CMAP) data (Xie and Arkin, 1997) were used in this study. Both datasets are monthly spanning from January 2003 to August 2012 at $1^{\circ} \times 1^{\circ}$ geographical latitude and longitude grid.

2.2 Flood observation data

Two flood datasets were used: (1) DFO (Brakenridge and Anderson, 2006) and (2) the US Geological Survey (USGS) Retrieve Summary of Recent Flood and High Flow Conditions (Hirsch and Costa, 2004). These datasets differ substantially in that the DFO is derived from news and governmental sources and hence mainly refers to large floods in denser-populated regions whereas the USGS reports are based on in situ stream gages. In addition, the DFO data cover the period from 1985 till present and the USGS data are available since October 2007.

DFO classifies a flood as “large” if a significant damage to structures or agriculture, human life loss and/or flood event of long duration. Since DFO data are mainly based on damage to infrastructure and loss of life as reported by media, its coverage is expected to bias towards the more densely populated regions and/or regions of interest for particular organizations. The DFO data were downloaded as a GIS vector dataset providing an outline of the area affected by a flood with such attributes as flood dates, duration, fatalities, primary country of flooding, etc. The data were further screened for quality control. For example, in several instances in 2006 and 2009 a mismatch was located between the assigned flood’s geographical coordinates and the primary country of flooding; these events were excluded from our analysis. Finally, vector maps of DFO flood events were rasterized to $1^{\circ} \times 1^{\circ}$ grids.

The USGS deploys 9044 gages in the continental US (Fig. 1) for flood monitoring. Each gage daily reports a flood as a flow overtopping the natural or artificial banks. A flood is further categorized into minor, moderate or major, with number of days in a month in each flood category also reported. Because significant difference exists in spatial scale between GRACE RFPI data and USGS gage based flood reports, the USGS data was aggregated into $1^\circ \times 1^\circ$ grid. First, to ensure statistical significance, all grid cells containing less than 5 USGS gage stations were excluded from the analysis (Fig. 1). For each of those grid cells with more than 5 stream gage stations, gage reports were combined by all the stations within the cell into a monthly flood coefficient X:

$$X = \frac{D_{\mathrm{mi}} + 5 \cdot D_{\mathrm{mo}} + 10 \cdot D_{\mathrm{ma}}}{N} \tag{1}$$

where N represents the total number of stations within a cell; D_{mi}, D_{mo} and D_{ma} are total numbers of days when the stations within a cell reported minor, moderate or major floods, respectively. Flood duration, geographical extent and flood stage are all taken into account in Eq. (1). Analyzing several events from the DFO database and the corresponding X coefficient estimated from Eq. (1), it was found that areas with cells that are flagged as flooded with X greater than 0.5 agreed well with the DFO flood report (Fig. 2). A value of 0.5 for the X coefficient indicates that within a grid cell, 50 % of the gages reported minor flood for 1 day, or 10 % of the gages reported moderate flood for 1 day, or 1 % of stations reported major flood for 1 day. In further analysis it was assumed that a grid cell is experiencing a large flooding if the X coefficient is greater than 0.5. In Eq. (1) weighs of 1, 5 and 10 were assigned to differentiate minor, moderate and major flooding. The exact values for weighting are not important in our analysis because the values of X estimated using different weighting are linearly related. For example, if a weighting scheme of 1, 2 and 3 is used, then a flood trigger would be $X \geq 0.1$.

2.3 Forecasting skill assessment

Forecasting skill is an overall measure of how well the previous forecasts were associated with previous observations (Murphy and Winkler; 1997). Receiver Operating

NHESSD
3, 6977–6996, 2015

Characteristics (ROC) (Fawcett, 2006) is commonly used as a method for testing the performance of a continuous index (such as RFPI) against binary observational data (e.g., flood or no flood). It uses a binary classifier that maps the index values below and above a certain threshold τ to the occurrence of an event. Since the exact threshold value is unknown a priori, the ROC analysis is performed for a range of possible threshold values. For each threshold, a pair of true positive rate (TPR) and false positive rate (FPR) was generated by constructing a contingency table (see Table 1). An ROC curve plots TPR vs. FPR for different thresholds and two additional points (0; 1) and (1; 1) are added to "anchor" the curve (see Fig. 3). On the ROC plot the 1:1 line represents the result of a random guessing.

The AUC (the Area Under Curve) is the area that resides beneath the ROC curve. AUC values greater than 0.5 correspond to better index performance with AUC = 0.5 related to no skill and AUC > 0.7 indicating a strong predictive skill (Morrison, 2005). In practice, the 0.6, 0.7, 0.8, and 0.9 AUC values are frequently used as the thresholds for fair, satisfactory, good, and excellent predictive skill. The optimal value of the classifier threshold τ can also be estimated from the ROC plot. Generally, the optimal threshold value is the one with the corresponding point on the ROC curve that is the closest to the (0, 1) point (Fig. 3).

3 Results

A satisfactory to good agreement was found between the RFPI and the observed floods from both the DFO and filtered USGS data for the conterminous USA; the AUC values was 0.75 for the comparison of RFPI with DFO flood observations and 0.72 when compared to USGS which indicates a strong predictive skill (Morrison, 2005). Figure 4 shows ROC curves for the comparison of RFPI with USGS flood observations from 2007 to 2012 and with DFO data from 2003 to 2012. Since DFO flood observations are biased towards high-damage and large-scale floods, the RFPI skill measured against this dataset is higher, as can be expected, in comparison with the USGS observa-

NHESSD
3, 6977–6996, 2015

tions. The optimal threshold values for τ are −0.4 and −0.3 respectively, depending on whether USGS or DFO data are compared to.

The validation against the USGS data has also demonstrated ability of the RFPI to estimate flood risks at a watershed level in large flat areas (Fig. 5), e.g. the Great Plains region, with AUC persistently exceeding the 0.7 strong predictive skill level. At the same time, we found that over the mountainous and coastal regions the RFPI has a limited ability of flood monitoring (Fig. 5). The resulting ROC curves have different shapes and the optimal threshold varies between −0.4 and 0.1 for different watersheds. The RFPI skill, however, varies over the seasons. For example, in the Larger Mississippi watershed (consisting of Upper and Lower Mississippi, Missouri, Ohio, Tennessee and Arkansas-Red-White watersheds – Fig. 6), AUC vary between 0.67 in winter period and 0.78 in summer. The October 2006 flood in the 783 000 km^2 Juba–Shabelle river basin shared between Somalia and Ethiopia was used as a case study to demonstrate the utility of the TWSA product for flood risk detection in developing countries. The flood caused by heavy rain had devastating consequences for these countries, becoming the most damaging flood in Eastern Africa in 50 years. In Ethiopia, over 150 people have died and over 122 500 were displaced (DFO database); in Somalia, over 80 people have died and over 299 000 were displaced. Figure 7 shows the RFPI for the Juba–Shabelle watershed for the months immediately preceding the flood (September, Fig. 7a) and the month of flood (October, Fig. 7b). Notice that the October RFPI flood risk predictions (based on September data) are well in agreement with the actual flood extent area (DFO database estimate). Figure 7c confirms this by demonstrating the time series of the water storage deficit in the watershed, with the significant drop in the available water storage capacity in the watershed in September, one month before the disaster.

4 Discussion

We found that the RFPI has a good predictive skill for flood monitoring, both at a national, watershed and a sub-watershed levels, especially in large river basins located over the flat areas such as the Mississippi river basin. Method's skill is significantly higher in summer period, when floods are mainly caused by heavy rainfall. During the cold period of the year, RFPI skill is relatively low as the method is over-sensitive to recent precipitation, while winter floods are primarily caused by the ice jams and snowmelt accumulated from the previous months. This additionally lowers RFPI skill during spring months. This limitation seems, however, relatively weak in developing countries, where floods are mainly caused by heavy rainfall events which account for greater damage and the most loss of life, as found through the DFO database. Modification of the method to include snowmelt is likely to improve its skill.

A potential weakness of the approach is linked to a 2012 update of the TWSA product. Multiple early studies demonstrated the utility of TWSA to detect the changes in water storage over land, e.g. over the world's major river basins (Schmidt et al., 2006; Yeh et al., 2006; Kim et al., 2009). In 2012, the new TWSA release 5 was distributed for immediate use to replace previous datasets (http://grace.jpl.nasa.gov/data/monthly-mass-grids/). Accordingly, the results reported in this paper were obtained using the updated version of the product. Test computations of flood risks using the previous version of TWSA were performed which provided similar results; however the overall correspondence between the results obtained with different versions of TWSA was not tested.

The GRACE-based RFPI is not free of limitations, e.g. associated with coarse time and spatial resolution of GRACE data, which makes the product unsuitable for forecasting local high-intensity events such as flash floods. Nevertheless, it has a unique ability to provide an insight on water migration within a region and, in combination with traditional methods of precipitation forecasting, increase warning time by a few weeks, while an advanced prototype of a flood warning system like EFAS produce probabilistic

NHESSD
3, 6977–6996, 2015

flood alerts with lead times of up to 10 days only. The comparison of the flood potential index against the backcast observations proves the proposed technique is valuable and might be crucial for the developing countries that have not yet developed national flood prediction and monitor systems. Most likely the integration of the gravitational anomaly based products with higher-resolution remotely sensed data, such as MODIS products used in the CRED flood monitoring system, will serve as a good addition to other flood detection methods. We see the product especially useful in developing countries with less dense hydrological monitoring networks and less advanced flood mitigation infrastructure.

Acknowledgements. The study was supported by NASA grant NNX10AH20G and UND Summer Graduate Research Professorship. The GRACE Release-5 10/2012 TWSA product was obtained from http://grace.jpl.nasa.gov/ the CPC Merged Analysis of Precipitation was obtained from http://disc.sci.gsfc.nasa.gov/giovanni DFO Global Archive of Large Flood Events data were obtained from http://www.dartmouth.edu/~floods/Archives/; the USGS Retrieve Summary of Recent Flood and High Flow Conditions was obtained from http://waterwatch.usgs.gov/

References

Adam, D., Gravity measurement: amazing GRACE, Nature, 416, 10–11, 2002.

Alexander, L. V., Zhang, X., Peterson, T. C., Caesar, J., Gleason, B., Tank, K., Haylock, M., Collins, D., Trewin, B., Rahimzadeh, F., Tagipour, A., Kumar, R., Revadekar, J., Griffiths, G., Vincent, L., Stephenson, D. B., Burn, J., Aguilar, E., Brunet, M., Taylor, M., New, M., Zhai, P., Rusticucci, M., and Vazquez-Aguirre, J. L.: Global observed changes in daily climate extremes of temperature and precipitation, J. Geophys. Res., 111, D05109, doi:10.1029/2005JD006290, 2006.

Bartholmes, J. C., Thielen, J., Ramos, M. H., and Gentilini, S.: The european flood alert system EFAS – Part 2: Statistical skill assessment of probabilistic and deterministic operational forecasts, Hydrol. Earth Syst. Sci., 13, 141–153, doi:10.5194/hess-13-141-2009, 2009.

Brakenridge, G. R., Anderson, E., Nghiem, S., Caquard, S., and Shabaneh, T. B.: Flood warnings, flood disaster assessments, and flood hazard reduction: the roles of orbital remote sensing, In 30th International Symposium on Remote Sensinf Environment, Honolulu,

HI, 10–14 November, Pasadena, CA: Jet Propulsion Laboratory, National Aeronautics and Space Administration, 2003.
Brakenridge, R. and Anderson, E.: MODIS-based flood detection, mapping and measurement: the potential for operational hydrological applications, Transboundary Floods: Reducing Risks Through Flood Management: Nato science series: IV: earth and environmental sciences, 72, p. 1, doi:10.1007/1-4020-4902-1_1.1-12, 2006.
Center for Research on the Epidemiology of Disasters: The OFDA/CRED International Disasters Database, available at: www.cred.be, last access: June 2013, 2013.
Chen, J. L., Wilson, C. R., Tapley, B. D., and Ries, J. C.: Low degree gravitational changes from GRACE: validation and interpretation, Geophys. Res. Lett., 31, L22607, doi:10.1029/2004GL021670, 2004.
Dai, A. and Trenberth, K. E.: Estimates of freshwater discharge from continents: latitudinal and seasonal variations, J. Hydrometeorol., 3, 660–687, 2002.
Groisman, P. Y., Knight, R. W., and Karl, T. R.: Changes in Intense Precipitation over the Central United States, J. Hydrometeor, 13, 47–66, doi:10.1175/JHM-D-11-039.1, 2012.
Groisman, P. Y., Knight, R. W., Easterling, D. R., Karl, T. R., Hegerl, G. C., and Razuvaev, V. N.: Trends in intense precipitation in the climate record, J. Climate, 18, 1326–1350, 2005.
Hagen, E. and Lu, X. X.: Let us create flood hazard maps for developing countries, Nat. Hazards, 58, 841–843, doi:10.1007/s11069-011-9750-7, 2011.
Hirsch, R. M. and Costa, J. E.: US stream flow measurement and data dissemination improve, Eos, 85, 197–203, 2004.
Hydrologic Information Center: NWS Annual Flood Loss Summary Reports To US Army Corps of Engineers, available at: http://www.nws.noaa.gov/hic/summaries/, last access: 12 November 2015.
Jain, S. K., Singh, R. D., Jain, M. K., and Lohani, A. K.: Delineation of flood-prone areas using remote sensing techniques, Water Resour. Manag., 19, 333–347, doi:10.1007/s11269-005-3281-5, 2005.
Kim, H., Yeh, P. J.-F., Oki, T., and Kanae. S.: Role of rivers in the seasonal variations of terrestrial water storage over global basins., Geophys. Res. Lett., 36, L17402, doi:10.1029/2009GL039006, 2009.
Larkin, K.: Pakistan's floods: is the worst still to come?, Nature News, doi:10.1038/news.2010.409, 2010.

NHESSD
3, 6977–6996, 2015

Evaluating flood potential with GRACE in the United States

T. Molodtsova et al.

Lombard, P. J.: Flood of April 2007 in southern Maine: US Geological Survey Scientific Investigations Report 2009–5102, 34 p., available at: http://pubs.usgs.gov/sir/2009/5102 (last access: 12 November 2015), 2009.

Luo, L. and Wood, E. F.: Monitoring and predicting the 2007 US drought, Geophys. Res. Lett., 34, L22702, doi:10.1029/2007GL031673, 2007.

Morrison, A. M.: Receiver operating characteristic (ROC) curve analysis of antecedent rainfall and the alewife/mystic river receiving waters, Boston, Massachusetts Water Resources Authority, Report ENQUAD 2005–23, 26 pp., 2005.

Murphy, A. and Winkler, R.: A general framework for forecast verification, Mon. Weather Rev., 115, 7, 1330–1338, 1987.

Proud, S. R., Fensholt, R., Rasmussen, L. V., and Sandholt, I.: Rapid response flood detection using the MSG geostationary satellite, Int. J. Appl. Earth Obs., 13, 536–544, 2011.

Ramillien, G., Cazenave, A., and Brunau, O.: Global time variations of hydrological signals from GRACE satellite gravimetry, Geophys. J. Int., 158, 813–826, doi:10.1111/j.1365-246X.2004.02328.x, 2004.

Reager, J. T. and Famiglietti, J. S.: Global terrestrial water storage capacity and flood potential using GRACE, Geophys. Res. Lett., 36, L23402, doi:10.1029/2009GL040826, 2009.

Reager, J. T. and Famiglietti, J. S.: Characteristic mega-basin water storage behavior using GRAC E, Water Resour. Res., 49, 3314–3329, doi:10.1002/wrcr.20264, 2013.

Scawthorn, C.: Modeling flood events in the US, Proceedings of EuroConference on Global Change and Catastrophe Risk Management, p. 7, IIASA, Laxenburg, Austria, 6–9 June, 1999.

Schmidt, R., Schwintzer, P., Flechtner, F., Reigber, Ch., Güntner, A., Döll, P., Ramillien, G., Cazenave, A., Petrovic, S., Jochmann, H., and Wünsch, J.: GRACE observations of changes in continental water storage, Global and Planet. Change, 50, 112–126, doi:10.1016/j.gloplacha.2004.11.018, 2006

Stephenson, D. B.: Use of the odds ratio for diagnosing forecast skill, Weather Forecast., 15, 221–232, 2000.

Tariq, M. A. U. R.: Risk-based planning and optimization of flood management measures in developing countries: Case Pakistan, PhD thesis, VSSD, TU Delft, Delft University of Technology, 2011.

Trenberth, K. E.: Changes in precipitation with climate change, Clim. Res. 47, 123–138, 2010.

NHESSD

3, 6977–6996, 2015

Evaluating flood potential with GRACE in the United States

T. Molodtsova et al.

Wang, Q., Watanabe, M., Hayashi, S., and Murakami, S.: Using NOAA AVHRR data to assess flood damage in China, Environ. Monit. Assess., 82, 119–148, 2003.
Xie, P. and Arkin, P. A.: Global precipitation: a 17 year monthly analysis based on gauge observations, satellite estimates, and numerical model outputs, B. Am. Meteorol. Soc., 78, 2539–2558, 1997.
Yeh, P. J-F., Swenson, S. C., Famiglietti, J. S., and Rodell, M.: Remote sensing of groundwater storage changes in Illinois using the Gravity Recovery and Climate Experiment (GRACE), Water Resour. Res., 42, W12203, doi:10.1029/2006WR005374, 2006.

NHESSD
3, 6977–6996, 2015

Table 1. Schematic contingency table for categorical forecasts of a binary event. The TRP, also called the hit rate or the probability of detection, is a relative number of times an event was predicted when it actually occurred; the FPR, sometimes referred to as the false alarm rate gives a relative number of times the event was predicted when it did not occur.

		Observed (DFO or USGS)	
		yes	no
Forecasted (RFPI)	yes	a (hit)	b (false alert, Type I error)
	no	c (miss, Type II error)	d (positive rejection)
		$\text{TRP} = a/(a+c)$	$\text{FPR} = b/(b+d)$

NHESSD
3, 6977–6996, 2015

Evaluating flood potential with GRACE in the United States

T. Molodtsova et al.

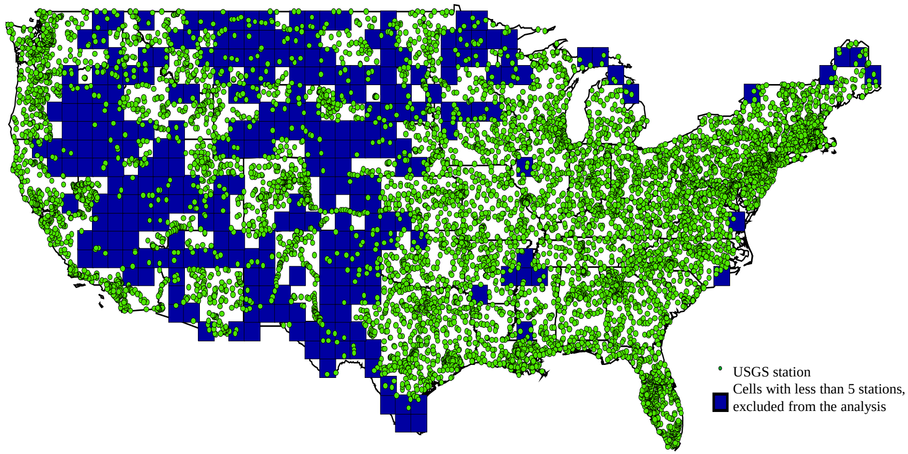

Figure 1. The distribution of the USGS stream gage stations (green dotes). The blue cells indicate those $1^{\circ} \times 1^{\circ}$ grids containing less than 5 stations.

NHESSD
3, 6977–6996, 2015

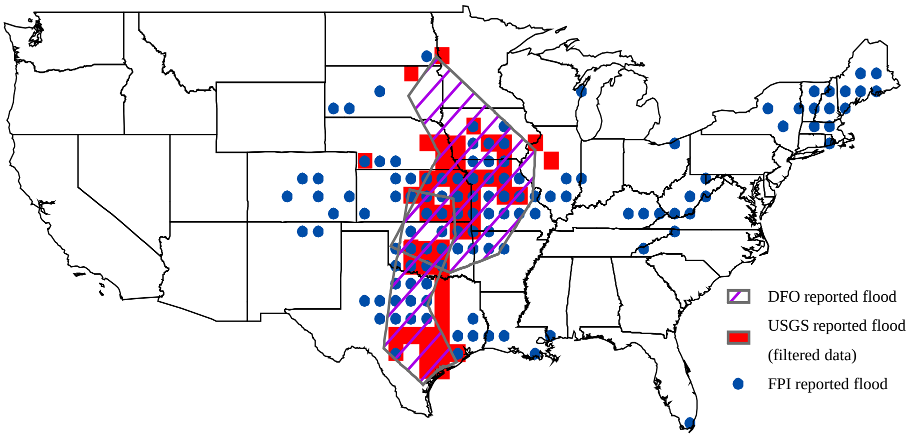

Figure 2. May 2007 with DFO reported flood, USGS reported flood (filtered data) and RFPI reported flood ($\tau = 0$).

NHESSD
3, 6977–6996, 2015

Evaluating flood potential with GRACE in the United States

T. Molodtsova et al.

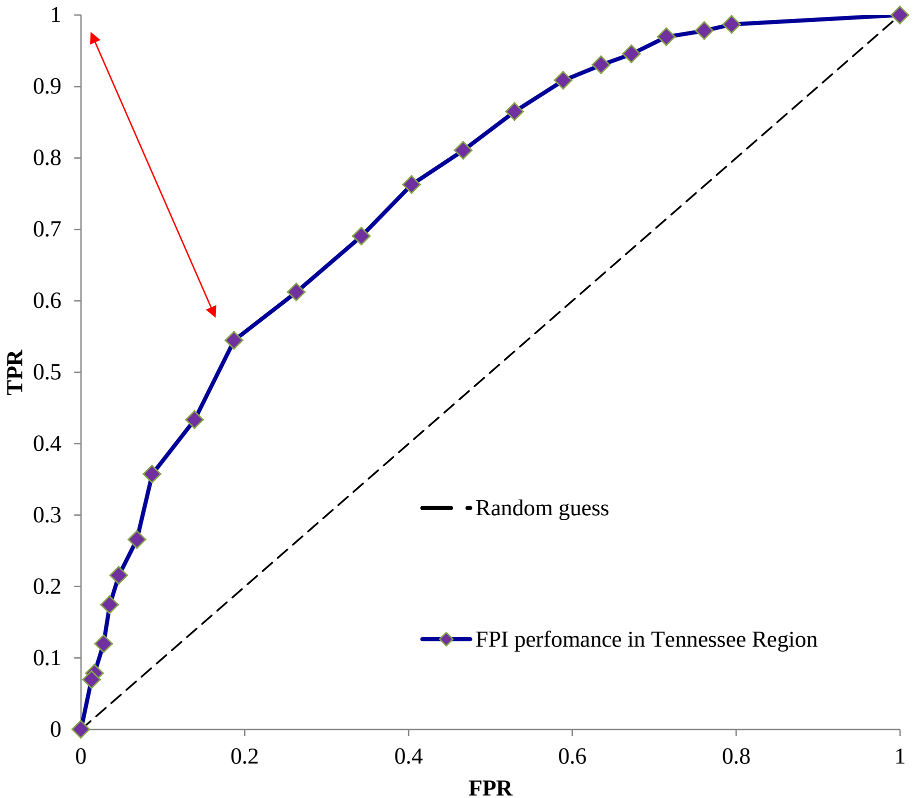

Figure 3. Sample ROC curve for the Tennessee watershed (purple). The markers represent different RFPI thresholds. The optimal value of the classifier threshold τ for this watershed is -0.1. The optimal threshold value must correspond to the point on the ROC curve, which is the closest to the (0, 1) point. The random guess line (black dashed line) follows the diagonal of the plot and has an AUC of 0.5.

NHESSD
3, 6977–6996, 2015

Evaluating flood potential with GRACE in the United States

T. Molodtsova et al.

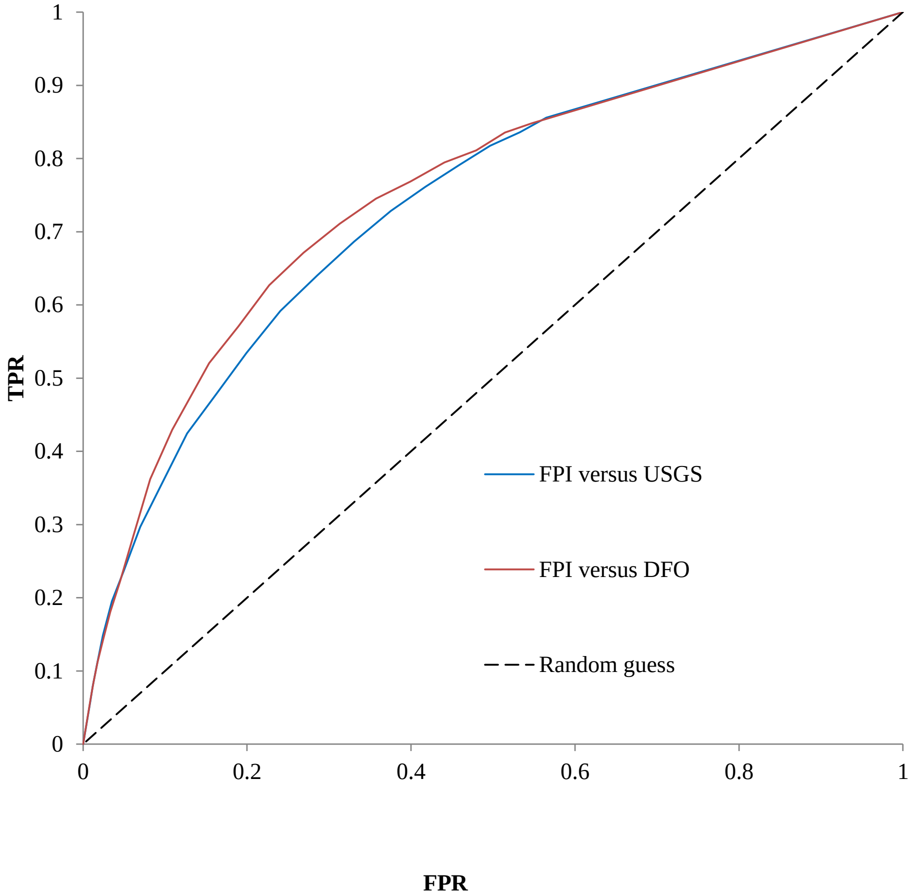

Figure 4. ROC curves for the comparison between the RFPI and the USGS- and DFO-reported floods.

NHESSD
3, 6977–6996, 2015

Evaluating flood potential with GRACE in the United States

T. Molodtsova et al.

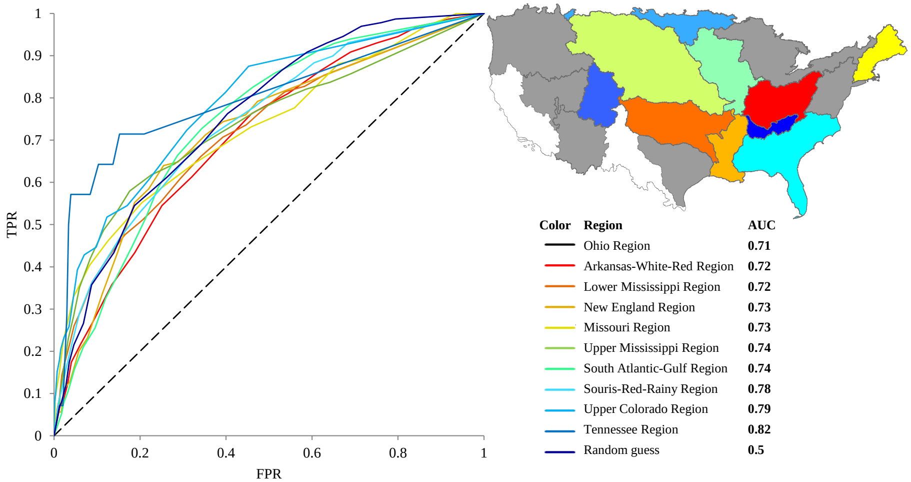

Figure 5. Evaluating RFPI predictive skills in major watersheds using USGS-reported floods ($X > 0.5$). **(a)** The ROC curves for each watershed and the corresponding RFPI AUC values. **(b)** Delineation of major watersheds. Rio Grande and California watersheds (in white) were excluded due to low number of floods. The watersheds that have RFPI AUC values less than 0.7 are in grey color (Lower Colorado, Texas-Gulf, Great Basin, Great Lakes, Mid Atlantic and Pacific Northwest).

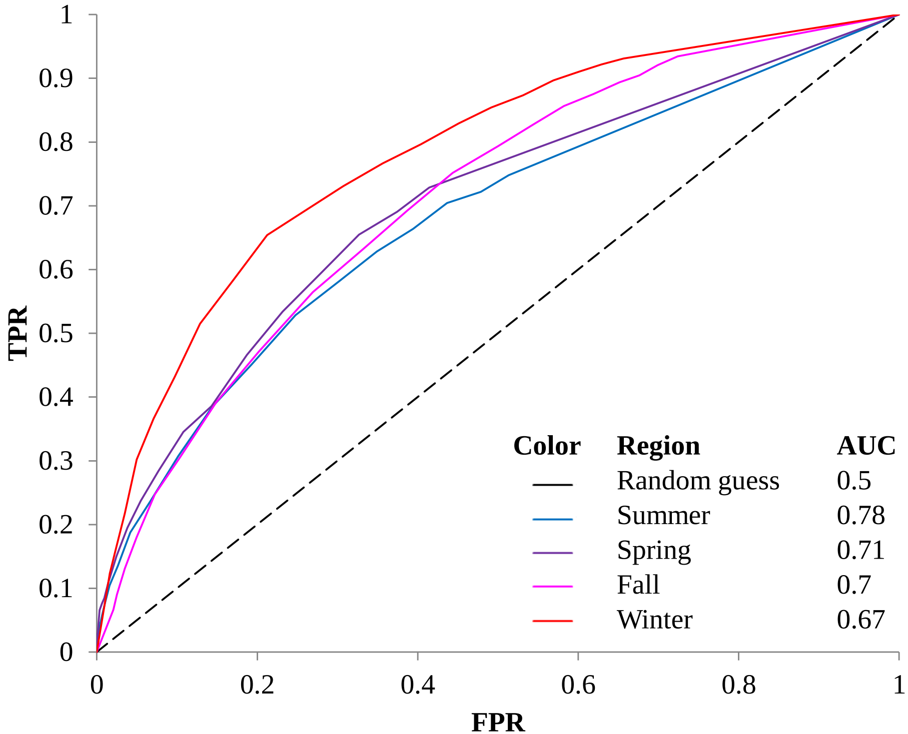

Figure 6. A comparison between the RFPI and the USGS-reported floods in the Mississippi river basin by the season.

NHESSD
3, 6977–6996, 2015

Evaluating flood potential with GRACE in the United States

T. Molodtsova et al.

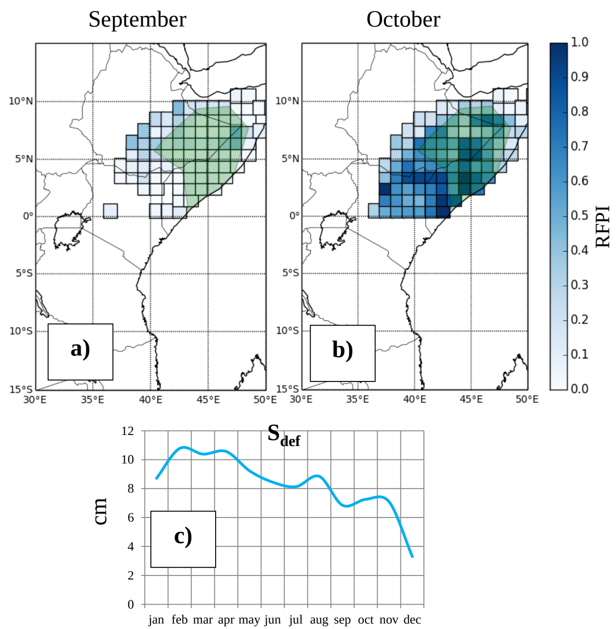

Figure 7. The 2006 flood in the Juba–Shabelle river basin **(a)** Grid cells with positive RFPI values in September, one month before the flooding, overlapped with the DFO flood polygon. **(b)** Grid cells with positive RFPI values in October, the flood month, overlapped with the DFO flood **(c)**. The storage deficit time series for the Juba-Shebelle watershed.

NHESSD

3, 6977–6996, 2015

Evaluating flood potential with GRACE in the United States

T. Molodtsova et al.